Energy Conversion and Management xxx (xxxx) xxxx

Contents lists available at ScienceDirect

Energy Conversion and Management

journal homepage: www.elsevier.com/locate/enconman

Nanofluid figure-of-merits to assess thermal efficiency of a flat plate solar collector

Elif Begum Elcioglu[a], Alper Mete Genc[b], Ziya Haktan Karadeniz[c], Mehmet Akif Ezan[d], Alpaslan Turgut[d,*]

[a] Eskisehir Osmangazi University, Sivrihisar Vocational School, Mechanics Program, Sivrihisar 26600, Eskisehir, Turkey
[b] Izmir Katip Çelebi University, The Graduate School of Natural and Applied Sciences, Department of Mechanical Engineering, Çiğli 35620, Izmir, Turkey
[c] Izmir Katip Çelebi University, Department of Mechanical Engineering, Çiğli 35620, Izmir, Turkey
[d] Dokuz Eylul University, Faculty of Engineering, Department of Mechanical Engineering, Tinaztepe Campus, Buca 35397, Izmir, Turkey

ARTICLE INFO

Keywords:
Solar collector
Nanofluid
Thermal efficiency
Figure-of-merit

ABSTRACT

The thermal system design strongly depends on material selection. Nanofluids offer design flexibility and fine-tuning of properties by incorporation of nanoparticles in base fluids. This flexibility is guided by particle-particle communication, which may be beneficial in creating ballistic routes in heat transfer but also detrimental due to affecting nanofluid properties. The transition of nanofluids to industrial use requires application-based examinations. For this purpose, different types of nanofluids were investigated in this work in terms of their thermal efficiency in a flat plate solar collector (FPSC) and some figure-of-merits (FOMs), under laminar and turbulent flow conditions. Investigation of both aims at clarifying the correlation between FOMs and FPSC thermal efficiency, and further reporting on the validity of FOMs in assessing thermal efficiency. Results indicate that nanofluids' eligibility as a heat transfer fluid depends on the flow condition, since a base fluid could outperform a nanofluid under turbulent flow. Nanofluid type and nanoparticle shape affects thermal performance, as suspensions of nanoplatelets/nanotubes in low concentrations ($<$ 0.04 vol%/0.25 vol%) are shown to outperform certain spherical metal-oxide nanoparticles ($<$ 3 vol%), according to some FOMs. It is shown that performance evaluation criteria (*PEC*), overall energetic efficiency, and energy ratio (*ER*) do not capture FPSC thermal efficiency trends, e.g., for graphene nanoplatelet nanofluid, as Mouromtseff number-based comparisons do for laminar and turbulent conditions. It must be highlighted that the FOM type to indicate thermal efficiency should be chosen depending on the application, and simultaneous consideration of thermal and hydrodynamic characteristics is required.

1. Introduction

In today's world, the main emphasis in energy industry lies on the concept of "sustainability" in energy applications. Plenty of Rooms at the Bottom are available, as stated by Richard P. Feynmann [1], at the enhanced surface-to-volume ratio of nanoparticles which bring about unique characteristics to base fluids when mixed with nanoparticles. Nanofluids [2] or nano-enhanced Heat Transfer Fluids (ne-HTFs) have been under research in a variety of heat transfer-based systems. This has been by necessity due to the poor thermal characteristics of most conventional HTFs, e.g., water, ethylene glycol, mineral oils, brines, etc. compared to solids. This fact highlighted the need for their replacement by ne-HTFs as a potential way to improve thermal performance of solar collectors, electronic cooling systems, nuclear reactor cooling schemes, refrigerators, and so forth.

Nanofluids thermal conductivity and heat transfer coefficient have been among the most investigated characteristics [3–5] in determining ne-HTFs' potential in various heating and cooling processes. Hydrodynamic and colloid state points of view show *per contra* that high viscosity of nanofluids cause increments in pressure drop, pumping power, operation cost, and nanoparticle sedimentation concerns to increase; as well as sometimes thermal performances no better than HTFs in turbulent flow and fully developed flow conditions [3,6–8]. Although the convective heat transfer coefficient and Nusselt number are important performance indicators, various types of figure-of-merits (FOMs) have been proposed to compare the heat transfer characteristics

* Corresponding author.
E-mail addresses: ebelcioglu@ogu.edu.tr (E.B. Elcioglu), zhaktan.karadeniz@ikcu.edu.tr (Z.H. Karadeniz), mehmet.ezan@deu.edu.tr (M.A. Ezan), alpaslan.turgut@deu.edu.tr (A. Turgut).

https://doi.org/10.1016/j.enconman.2019.112292
Received 1 August 2019; Received in revised form 11 November 2019; Accepted 12 November 2019
0196-8904/

Nomenclature

Symbols

c_p	Specific heat capacity [J kg^{-1} K^{-1}]
C	Enhancement coefficient
df	Degree of freedom
D	Pipe diameter [m]
Δp	Pressure drop [Pa]
H	Test hypothesis
ΔT	Temperature difference [K]
Eu	Euler number
h	Heat transfer coefficient [W m^{-2} K^{-1}]
k	Thermal conductivity [W m^{-1} K^{-1}]
$\dot{m}$	Mass flow rate [kg s^{-1}]
Mo	Mouromtseff number
Nu	Nusselt number
p	Significance
Re	Reynolds number
U	Fluid mean velocity [m s^{-1}]
$\dot{V}$	Volumetric flow rate [m^3 s^{-1}]

Greek symbols

ρ	Density [kg m^{-3}]
μ	Dynamic viscosity [kg m^{-1} s^{-1}]
φ	Nanoparticle concentration

Subscripts

0	Base fluid, null (hypothesis)
a	Alternative (hypothesis)
nf	Nanofluid
bf	Base fluid
p	Particle

of HTFs. One of the most earliest FOM definition is the Mouromtseff number (*Mo*) [9] that has been used to compare heat transfer capabilities of HTFs in laminar and turbulent flow conditions. Another FOM is defined as the ratio of viscosity enhancement and thermal conductivity enhancement coefficients [10], valid in the case of fully developed laminar flow. Sekrani et al. [11] suggested two different types of FOMs to compare the heat transfer capability of nanofluids as the performance evaluation criterion, i.e., *PEC*, [12] and overall energetic efficiency.

Nanofluid's usefulness and transition to industrial applications require in-depth systematic investigations, specifically on thermophysical properties; safety, health and environment issues [13]; and proper FOMs to describe nanofluid's effectiveness. Apart from the thermal or hydrodynamic indicators, price-related indices were also used as signals to predict the extent of the nanofluid use. Alirezaie et al. [14] stated that *Mo* was not a suitable criterion for efficiency (based on the Nusselt number and friction factor) determination for MWCNT, DWCNT, Ag and MgO nanofluids. They compared these nanofluids in terms of an efficiency-price index (*EPI*), i.e., *EPI* ∝ (efficiency) / (price). Results revealed that MgO-water nanofluids *EPI* were the highest under turbulent flow, while these samples' efficiencies were mostly the lowest among the HTFs studied. Allouhi et al. [15] used the relative heat transfer coefficient as a FOM for Therminol VP-1 based CuO nanofluid in a parabolic trough collector system. Yasinskiy et al. [16] evaluated the efficiency of low concentration HTFs containing a eutectic mixture of C_2H_{10} and $C_{12}H_{10}O$ as base fluid and TiO_2 nanoparticles in concentrated solar power plants via Dittus-Boelter correlation as a FOM. Their results revealed an increase in FOM with increased temperature and effective nanoparticle fraction. Gómez-Villarejo et al. [17] evaluated C_2H_{10} and $C_{12}H_{10}O$ eutectic mixture based Ag nanofluid and employed Dittus-Boelter correlation as a FOM in a concentrated solar power system. Their results have shown a non-monotonic change of FOM with temperature, while it increased with nanoparticle fraction.

As investigations on nanofluid integrated solar energy applications emerge, different nanofluid types including Al_2O_3 [18–24], Cu [25], CuO [18,26–28], SiO_2 [29], TiO_2 [30,31], Al_2O_3 with TiO_2 (hybrid) [32], CeO_2 [33], MWCNT [34], graphene nanoplatelet [35], MgO with MWCNT and CuO with MWCNT (hybrid) [36], WO_3 [37] nanoparticles' suspensions have been under focus for their suitability and efficiency. Solar energy systems are among the most probable systems where nanofluids would be utilized in the near-future. Literature highlights the potential of nanofluids in solar applications, as working fluids and as volumetric absorbers. Flat Plate Solar Collectors (FPSC's) as one of the most cost-effective solar energy systems, Direct Absorption Solar Collectors (DASC), and solar-photovoltaic (PV) systems have been studied for possible nanofluid use, rather than pure fluids. For example, it has been shown for a DASC that a graphite ne-HTF of 0.3 vol% had higher absorbance and lower reflectance than those of the bulk graphite as the absorbing medium [38], and a carbon black-EG medium outperformed its base fluid in terms of the absorption capacity and photo-thermal conversion efficiency [39]. Improvements in optical properties, if and when combined with improved thermal character (i.e., improved thermal conductivity as well as increased density - specific heat product) are expected to dominantly reflect in overall thermal efficiency. It was concluded in the review by Sarsam et al. [40] that the use of carbon-based nanoparticles dispersion in water at low concentrations would be a promising choice as an HTF in an FPSC system due to enhanced efficiency, decreased pumping power penalties and instabilities. In addition to FPSC systems, nanofluids are under research as potential volumetric absorbers in Direct Absorption Solar Collector (DASC) systems [41]. It is known that [40] viscous losses increase at higher flow rates for ne-HTF's. Since the pumping power adversely affects FPSC thermal efficiency, at the turbulent flow conditions water becomes more efficient than water-based Al_2O_3 ne-HTF in the working and design conditions. Eltaweel and Abdel-Rehim [42] experimentally compared the efficiency of water-based MWCNT ne-HTF's for thermosiphon and forced-circulation FPSC systems, and stressed that using the MWCNT-water nanofluid exhibited a greater impact in natural convection based system when compared against the forced-circulation system. Verma et al. [43] presented the efficiency-flow rate relation for low concentration MgO-water nanofluids and identified that there was an optimum mass flow rate point at which the efficiency was maximized. Beyond this rate, the efficiency was observed to be decreased. These studies highlight the advantage framework of nanofluids, which depends strongly on the flow regime. Verma et al. [44] experimentally investigated the feasibility of water-based Al_2O_3, TiO_2, SiO_2, CuO, graphene, and MWCNT nanofluids. Their results indicated that the collector efficiency was the highest for MWCNT (with the highest thermal conductivity and the lowest viscosity), followed by graphene, CuO, Al_2O_3, TiO_2, and SiO_2. Exergy efficiency decreased due to increasing in entropy generation caused by irreversible heat energy at high flow rates.

The lack of studies assessing the validity of different FOMs on foreseeing the overall thermal performance with nanofluids is a knowledge gap in the literature. It is necessary to assess whether FOMs (which are easier to obtain than to perform an in-depth thermal modeling for the system) are adequate measures to conclude ne-HTFs benefits / drawbacks in a certain heat transfer application. The focus of this work is the evaluation of the effectiveness of water-based Al_2O_3, TiO_2, SiO_2, polystyrene, graphene nanoplatelet (GNP), and SWCNT nanofluids in a Flat Plate Solar Collector (FPSC) by calculating a number of FOMs, and further investigating the thermal efficiency. The question to be answered in the end is "*Are FOMs proper indicators of FPSC's thermal performance*?".

2. Materials and methods

This work has a three-fold purpose: *(i)* calculation of FOMs for nanofluids studied, *(ii)* comparison of these FOMs with the FPSC thermal efficiency in both laminar and turbulent flow conditions, and *(iii)* evaluation of some FOMs in terms of their representability of thermal efficiency. In Section 2.1., the FOMs employed in this work are summarized where some explanations on which properties they depend on and how they are advised to be calculated are explained. Section 2.2. provides details of the solution procedure.

2.1. Performance measures employed in this work

Mouromtseff number (*Mo*) as a non-dimensional parameter has been used to evaluate the thermal performances of traditional HTF's, while *Mo* ratio (Mo_{nf} / Mo_{bf}) is used in comparing overall effectiveness of a candidate nanofluid against its base fluid. As defined in Eq. (1a), *Mo* depends on density, heat capacity, dynamic viscosity, and thermal conductivity [45] of an HTF and is valid in case of fully developed flow inside a circular pipe,

$$Mo = \frac{\rho^a k^b {c_p}^d}{\mu^e} \tag{1a}$$

where *a*, *b*, *d*, and *e* are determined by using an appropriate Nusselt number for the selected heat transfer application. For all convective heat transfer modes, flow regimes, and boundary conditions, the influence of thermal conductivity is greater than that of viscosity on *Mo*, i.e, $b > e$ [46]. Eq. (1a) can be solved for a nanofluid and a base fluid, and their ratio (Mo_{nf} / Mo_{bf}) defines the ratio of the convective heat transfer coefficients at constant velocity [45]. Yu et al. [45] stated that a *Mo* based comparison results in quite accurate performance comparisons for nanofluids. For laminar flow in a straight pipeline, either with constant wall temperature or heat flux, Nusselt number converges to a constant value for the fully developed conditions. That is, *Mo* ratio is defined as:

$$Mo_{ratio} = \frac{Mo_{nf}}{Mo_{bf}} = \frac{h_{nf}}{h_{bf}} = \frac{k_{nf}}{k_{bf}} \tag{1b}$$

In general, the specific heat and density are obtained via classical mixture rules. On the other hand, accuracy in thermo-physical property measurements is of critical importance [47] in evaluating realistic *Mo* values. The expression of Garg et al. [48] on the discrepancy between theoretical and experimental thermal conductivity and viscosity values of CuO-EG nanofluids is a good example of this issue. It is imperative to use representative data to conclude for effectiveness and further in the design of energy harvesting systems [49]. Another FOM compares the viscosity enhancement against the thermal conductivity enhancement of nanofluids, as:

$$\frac{C_\mu}{C_k} = \frac{(\mu_{nf} - \mu_{bf})/\mu_{bf}}{(k_{nf} - k_{bf})/k_{bf}} \tag{2a}$$

assessing benefits of the use of nanofluids in for fully developed laminar flow, once the criterion in Eq. (2b) is satisfied [10],

$$\frac{C_\mu}{C_k} < 4 \tag{2b}$$

This FOM implicitly compares the nanofluid and its base fluid regarding the relative differences between the thermal conductivities and viscosities [50]. While the increase in thermal conductivity is desired to be maximized and viscosity enhancement is desired to be minimized for convective heat transfer applications; lubrication applications favor increase in both [46]. While Eq. (2) considers advantages in thermal characteristics along with viscosity increase, *PEC* (Eq. (3a)) [12] provides a more in-depth comparison based on transferred heat and pumping power, for laminar and turbulent flow,

$$PEC = \frac{\dot{m} c_{p,nf} \Delta T}{\dot{V} \Delta p} \tag{3}$$

where $\dot{m}$ and $\dot{V}$ are the mass and volume flow rates, while ΔT and Δp respectively stand for temperature and pressure differences between outlet and inlet pipe sections. Another FOM is the overall energetic efficiency, introduced by Sekrani et al. [11]. The heat transfer improvement and the pressure drop penalty can be gathered to form a comparison based on overall energetic efficiency η, as:

$$\eta = \frac{Nu \Delta p_0}{\Delta p Nu_0} \tag{4}$$

where subscript 0 represents quantities evaluated for the case of $\varphi = 0\%$, i.e., base fluid. This merit is denoted as η herein, in order not to be confused with the FPSC thermal efficiency. Finally, based on the Nusselt number and Euler number, an Energy Ratio (*ER*) can be defined, as indicated by Vajjha and Das [51] as a FOM. Here, the *ER*, *Nu,* and *Eu* numbers are defined as:

$$ER = \frac{Nu}{Eu}, \; Nu = \frac{hD}{k}, \; Eu = \frac{\Delta p}{\rho U^2} \tag{5}$$

The *ER* provides a thermal-hydrodynamic flow characteristic comparison, which takes into account the advantages of high heat transfer coefficient (thus high *Nu*) and disadvantages of viscous losses with nanofluids, compared to pure fluids, as in Eq. (4), and partially as in Eq. (3).

2.2. Methodology

The current work is based on the early work of authors [23] about numerical investigation of an FPSC under real weather conditions, for which the transient solar irradiation and ambient temperature data were defined according to the monthly average daily weather data of Izmir, Turkey [23]. The modeled FPSC contains a 3.2 mm thick transparent glass cover, a 1.8 mm thick Cu absorber, and Cu tubes of 8.81 mm to circulate the HTF [23]. A transient code was developed by the authors to evaluate the thermal performance of the FPSC. The details of the validation procedure and the transient variations are represented in the previous work [23]. In the current work, authors extended the analyses by considering various water-based ne-HTFs which include Al_2O_3, TiO_2, SiO_2, polystyrene, GNP, and SWCNT nanoparticles, and compared the findings of thermal efficiency with different performance measures (FOMs) to assess the thermal performance of the FPSC. Another objective of this work is to assess the representability of the selected FOM's in rating the investigated HTFs as advantageous/disadvantageous, and their individual benefits in comparison to the actual FPSC thermal efficiency with these HTFs. This task is performed by means of a statistical procedure. The framework of the numerical solution method and the methodology of the statistical analysis are provided in the Supplementary Material.

3. Results

Solar radiation harvesting via an FPSC with different ne-HTF's are evaluated, and results are shown for *(i)* water-based Al_2O_3, TiO_2, SiO_2, polystyrene, GNP and SWCNT nanofluids in terms of thermal efficiency and detailed FOM based comparisons, and *(ii)* FPSC thermal efficiency-FOM comparison, statistically.

3.1. Thermal efficiency of Water-Based Al_2O_3, TiO_2, SiO_2, Polystyrene, graphene and SWCNT nanofluids

The ne-HTF's considered in this work are water-based Al_2O_3 nanofluids (1–3% vol.) whose thermal conductivity and viscosity data were taken from [52] (herein referred to as Al_2O_3 (I)); TiO_2 nanofluids (1–3% vol.) (data taken from [53]); SiO_2 (0.09–1.81% vol.), polystyrene (0.5%, 1% vol.) and Al_2O_3 (herein referred to as Al_2O_3 (II)) nanofluids (0.5%, 1% vol.) (data taken from [54]); GNP nanofluids (0.01–0.04% vol.) (data taken from [55]); and SWCNT nanofluids (0.05–0.25% vol.) (data taken from [56]). In the analyses, mass flow rates were set as 0.008 kg/s for laminar flow and 0.06 kg/s for turbulent flow, and the thermophysical properties were evaluated at 25 °C. The methods used in measurements as well as experimental accuracy levels reported by [52–56] are provided in the Supplementary Material. Investigation of water-based ne-HTF's is of great importance since water is one of the most commonly used and investigated types of HTF in FPSC's. The main contribution of this work is the use of experimental data for thermal conductivity and viscosity of the materials in calculation of FPSC thermal efficiency and FOM's, as classical models have limited use and provide erroneous results when extrapolated to larger parameter ranges. Mondragón et al. [57] stated that when studying thermal efficiency, incorporating thermo-physical property data from theoretical predictions failed at certain conditions since the applicability of these models is limited to certain nanoparticle fractions and definite shapes. They used experimental thermal conductivity, viscosity, and specific heat nanofluid data in their analyses, along with density data computed by using the mixture rule.

The thermal efficiency of the FPSC in October for laminar and turbulent flow with water-based nanofluids are compared respectively in Fig. 1 and Fig. 2. It is observed independent of the HTF that efficiency increases as the flow rate increases due to the reduced thermal resistance between the HTF and the tube wall at higher *Re*. Nanoparticles' presence in HTF's alters thermo-physical properties, and the critical mass flow rate for laminar to turbulent flow transition becomes different for ne-HTF's than that for their pure fluid counterparts. While water enters turbulent flow regime at 0.016 kg/s, ne-HTF's are in laminar condition at this rate, and exhibit a lower convective heat transfer coefficient. The ne-HTFs enter the turbulence for flow rates $>$ 0.016 kg/s. This highlights that the viscosity of ne-HTF's is a determining factor not only for the pumping power, but also on the flow type and characteristics. In turbulent region, nanoparticle loading has a negative impact on thermal efficiency for flow rates $>$ 0.016 kg/s. As outlined by [58], while increasing nanoparticle concentration increases the heat transfer coefficient, it simultaneously causes increased pumping power penalty.

When different nanofluids are compared, it is seen that the thermal efficiency of FPSC depends strongly on HTF thermo-physical properties. The thermal efficiency of base fluid (water) is 72.5% for laminar and 83.94% for turbulent flow. Fig. 1 shows increasing thermal efficiencies for laminar flow by increasing nanoparticle fraction except for SiO_2 and polystyrene nanofluids. This opposite dependence is due to the low thermal conductivity of SiO_2 and polystyrene; while for the other cases considered, thermo-physical properties increase as the nanoparticle content increases. Results also reveal that, thermal efficiency does not change considerably with nanotube fraction for SWCNT-H_2O nanofluid.

FPSC thermal efficiencies are given in Fig. 2 for turbulent flow, which are determined to be negatively correlated to nanoparticle fraction. Although most nanofluids possess higher thermal conductivity than that of base fluids; the advantage of high thermal conductivity may lose its significance at higher *Re* since the convective thermal resistances reduce significantly compared to the total thermal resistance across the FPSC. Efficiency trends are not straightforward for spherical and non-spherical nanoparticles' nanofluids (i.e., GNP and SWCNT). This result is due to the fact that SWCNT and GNP nanoparticles suspensions, although low in concentration, possess high thermal conductivity, while their viscosities are not as much enhanced. This causes the pump power penalty to be small compared to suspensions with higher nanoparticle loading, and leads to increased thermal efficiency in turbulent flow with increased nanoparticle fraction. As most of the theoretical models fail to explain particle-shape related effects on thermo-physical properties, necessity and importance of use of experimental data for platelet and cylindrical-shaped nanoparticles' suspensions can be seen.

Apart from thermal efficiency, the utility of a FPSC can be evaluated via the fluid outlet temperature. Fig. 3 depicts the outlet temperatures of the ne-HTFs considered in this work for laminar and turbulent flow conditions. It is seen that outlet temperatures are higher for laminar flow when compared to those for turbulent flow, and apart from the thermal efficiency, this may be an advantage if the target application is to use higher temperature.

3.2. Figure-of-Merits (FOMs) for different nanofluids under laminar and turbulent flow regimes

In this work for the sake of completeness, a number of FOMs that are applicable both to laminar and turbulent flow regimes are considered. These FOMs are *Mo* ratio, C_μ / C_k, PEC, η, and *ER*.

The *Mo* ratios are presented for laminar (Fig. 4) and turbulent (Fig. 5) flow. In Fig. 4, *Mo* ratio increases with increasing particle concentration, except for SiO_2 and polystyrene nanofluids. This finding is in agreement with the thermal efficiency results (see Fig. 1). Thermal conductivity of SiO_2 and polystyrene nanofluids decrease with increasing particle concentration [54], negatively affecting thermal

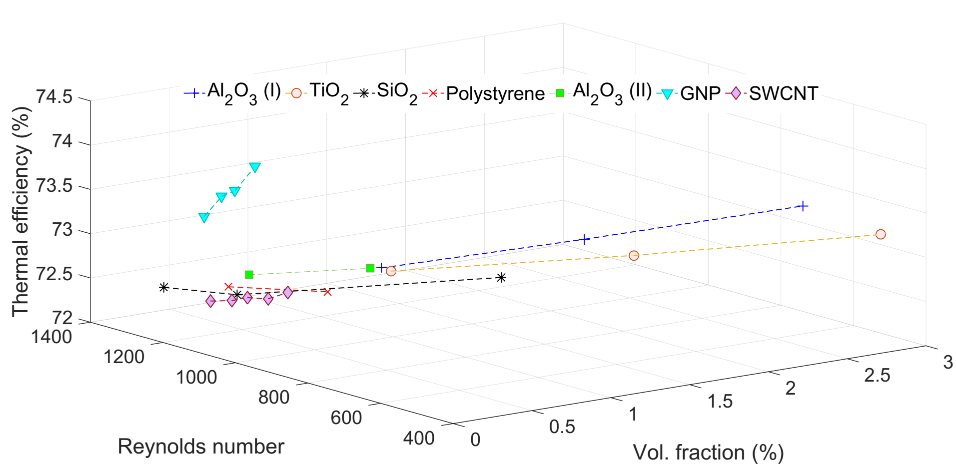

Fig. 1. FPSC thermal efficiencies for laminar flow [49].

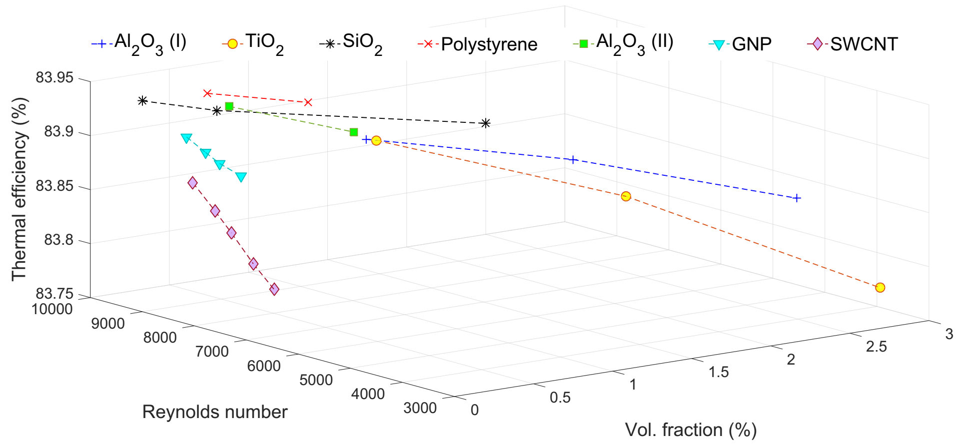

Fig. 2. FPSC thermal efficiencies for turbulent flow.

conductivity dependent FOMs for them at higher nanoparticle loadings. The opposite is the case for the ne-HTFs whose thermal conductivities increase with particle concentration. It can be concluded from Fig. 4 that, based on the *Mo* ratios, nanofluids except for SiO_2 and polystyrene nanoparticles suspensions are efficient HTFs for laminar flow. *Mo* ratio results are found compatible with thermal efficiencies for laminar flow.

As defined in Eq. (1), *Mo* ratio depends on thermophysical properties of the HTFs while two of these properties, i.e., thermal conductivity and viscosity, are more critical than others. Ensuring $Mo_{nf}/Mo_{bf} > 1$ is required to conclude for a specific nanofluid to replace its base fluid counterpart [58]. For this case the viscosity of nanofluids must be lower, and the thermal conductivity must be higher than those of the base fluid. Fig. 5 shows that Mo_{nf}/Mo_{bf} generally decreases with increasing particle concentration for turbulent flow. This can be explained with the effect of the relative viscosity, which becomes more determining than the relative thermal conductivity for the calculation of *Mo* ratio (Eq. (1)). On the other hand, GNP and SWCNT based nanofluids have different characteristics, that possibly arise from their thermo-physical properties, and their non-spherical particle shapes. At low concentrations, very high thermal conductivity values have been obtained for GNP and SWCNT nanofluids, which causes an increased *Mo* ratio for increasing concentrations for turbulent flow. Overall, *Mo* ratio results are compatible with findings of the thermal efficiency for laminar and turbulent flow cases.

In brief, it can be inferred from Fig. 4 and Fig. 5 that increased particle concentration results mostly in performance augmentation for laminar flow and may lead to a performance reduction in turbulent flow. A similar conclusion was made by [50] based on the *Mo* ratio that higher concentrations were advantageous/disadvantageous for laminar/turbulent flow of 2–4% Al_2O_3 nanofluids.

Fig. 6 compares C_μ/C_k values, presenting a direct comparison of thermal and hydrodynamic reflections of nanoparticle addition into pure HTFs. This ratio is commonly used in the literature for laminar flow, while Sekrani et al. [11] used this merit for turbulent flow. Fig. 6 shows different variations for each nanofluid group. According to Eq. (2), when the relative thermal conductivity is too small, C_μ/C_k can easily raise above the limit, 4, for which Prasher et al. [10] specified the bound for nanofluids' effectiveness with this FOM. The negative C_μ/C_k values in Fig. 6 should be noted, which is caused by the reduced thermal conductivity of the nanofluid compared to that of water. This outcome reduces the effectiveness of C_μ/C_k as a FOM in demonstrating nanofluids' effectiveness.

Another performance index, performance evolution criterion (*PEC*) ratio ($PEC_{ratio} = PEC_{nf}/PEC_{bf}$) is shown in Fig. 7 and Fig. 8 for laminar and turbulent flow conditions, respectively. $PEC_{nf}/PEC_{bf} < 1$ implies that the energetic performance of a nanofluid is not better than that with the pure fluid. Strong increase of dynamic and kinematic viscosity of nanofluids is an important concern which causes increase in pressure losses. Consequently, if and once the viscosity enhancement is too much, even if a heat transfer enhancement is observed, the required power for the pumping is increased compared to the base fluid, leading to an unfavorable energetic balance. It may be inferred from Eq. (3)

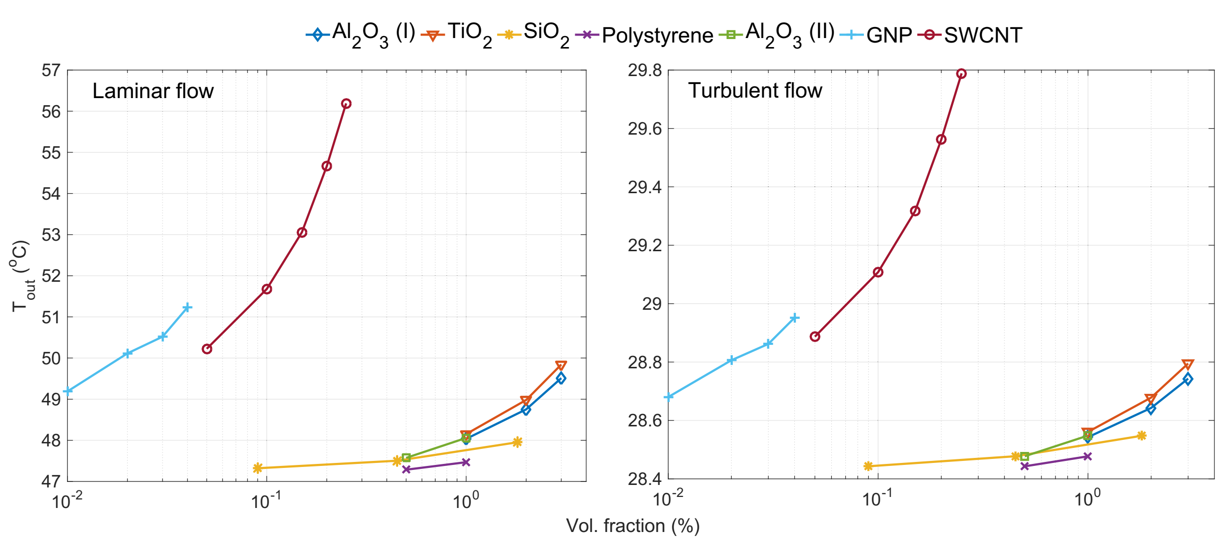

Fig. 3. Fluid outlet temperatures for laminar and turbulent flow.

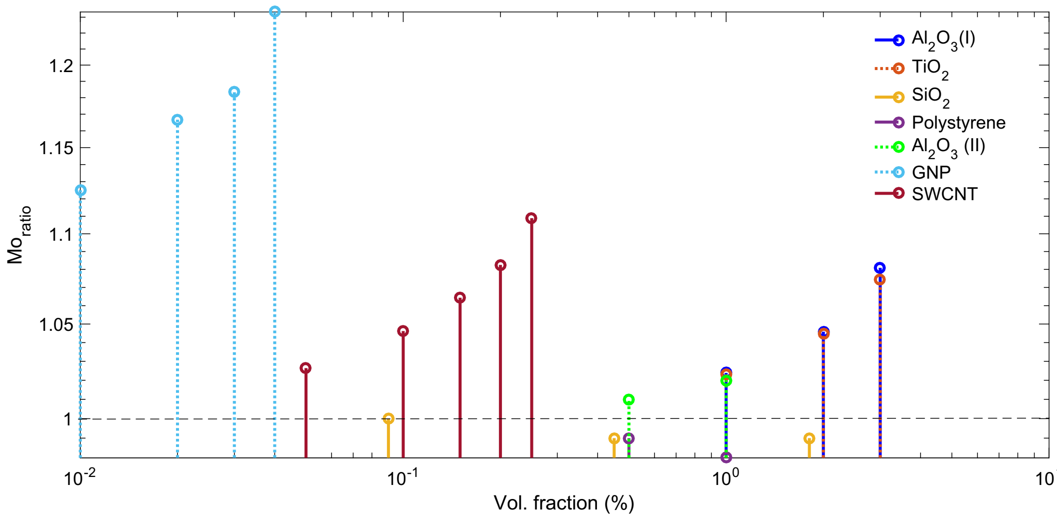

Fig. 4. *Mo* ratios for laminar flow [49]. The horizontal dashed line depicts the *Mo* ratio of water.

that density is also crucial in *PEC* evaluation, such that nanofluids with high-density exhibit high *PEC* values. When the thermal efficiency results in Fig. 1 are compared to those in Fig. 7, it is seen that the *PEC* ratios are not compatible with thermal efficiency results under laminar flow conditions. As opposed to all the ne-HTFs considered in this work, SWCNT/water nanofluids *PEC* ratios increase with increasing particle concentrations, since the increase in their viscosity is low, causing a less pronounced increase in the pressure drop, thereby increasing the *PEC* ratio. From a nanoparticle fraction based comparison point of view, the *PEC* results for turbulent flow are compatible with thermal efficiency except for the SWCNT-water nanofluids, since PEC_{ratio} values increase as the nanoparticle loading increases. This behavior is caused by lower pressure drops and higher thermal characteristics of SWCNT ne-HTF's, compared against those of studied ne-HTF's.

Another FOM presented by Sekrani et al. [11], η, allows for a comprehensive comparison by considering heat transfer and pressure drop penalty (see Eq. (4)). For fully developed laminar flow, the Nusselt number is constant (3.66) for constant surface temperature. In this case, Eq. (4) depends only on pressure drop. In Fig. 9 and Fig. 10, overall energetic efficiency decreases with increasing particle concentrations for all nanofluids, except for SWCNT nanofluids in laminar flow. The reason for the decrease in η with increasing concentration is the increase in viscosity at higher concentrations for the nanofluids with metal-oxide, SiO_2 and polystyrene nanoparticles, and GNP's, causing the pressure drop to increase and negatively influencing η. Overall, the η results are determined compatible with thermal efficiency results for only turbulent flow conditions, apart from the SWCNT case.

Another effectiveness comparison may be made by combining heat transfer and pressure loss that result from the use of a certain type of HTF. By employing *Nu* as a heat transfer indicator and *Eu* as a pressure drop indicator, Vajjha and Das [51] pointed out to the use of *Nu* / *Eu*, termed the Energy Ratio (*ER*). For the HTF's studied in this work, the *ER* values are shown in Fig. 11 for laminar flow, and in Fig. 12 for turbulent flow. A clear finding from Fig. 11 and Fig. 12 would be the increase of *ER* when the process takes place in turbulent flow in comparison to laminar flow. The results for the *ER* can be interpreted along with the results of η (Fig. 9 and Fig. 10), where the amount of transferred heat is also incorporated in with the Nusselt number. From the definition of *Nu*, if the extent of the enhancement in thermal conductivity is greater than that in the heat transfer coefficient, nanoparticle fraction – *Nu* relationship would not show a monotonous and the most promising trend. The relative changes in these characteristics may reflect in increased or decreased *Nu* and *Eu*, and thereby in the *ER*.

It is determined that the *ER* is the highest for water, which is followed by 1% polystyrene, and low concentration SiO_2 and Al_2O_3 (see Fig. 11). Since *Nu* is constant for laminar flow, *ER* comparisons are

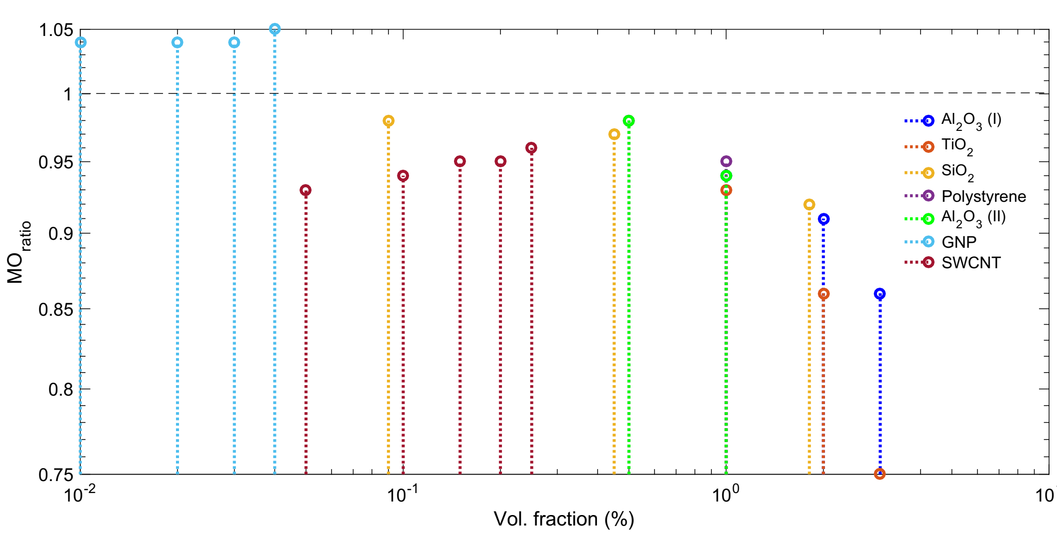

Fig. 5. *Mo* ratios for turbulent flow. The horizontal dashed line depicts the *Mo* ratio of water.

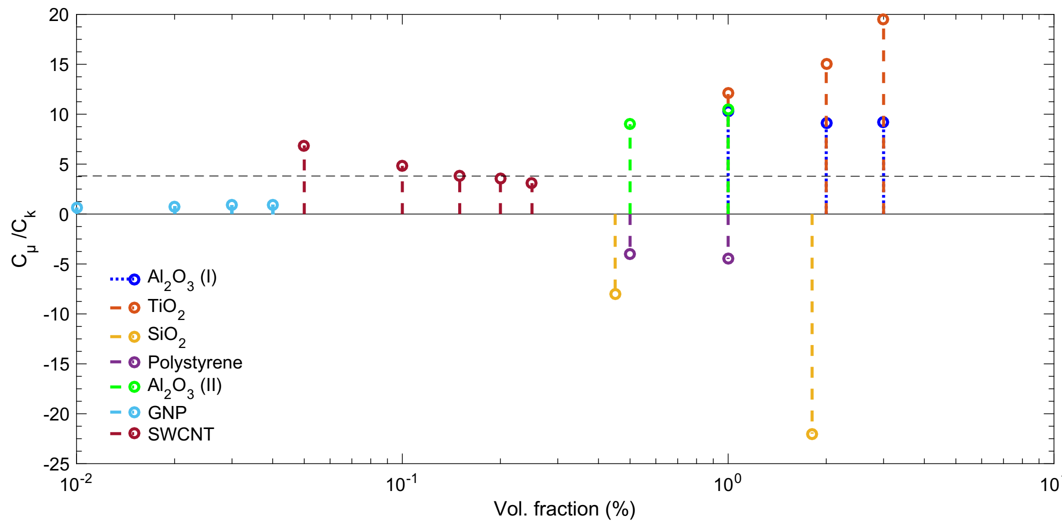

Fig. 6. C_μ / C_k, irrespective of the flow regime. The horizontal dashed line depicts the C_μ / C_k = 4 limit.

directly related to *Eu*, which is directly proportional to the pressure drop. These ne-HTF's cause the lowest pressure drops among the HTF's considered in this work. Although water-based polystyrene and SiO_2 nanofluids were considered not beneficial in terms of their C_μ / C_k values, here the *ER* based comparison yields a different point of view, from thermal conductivity (conduction) – heat transfer coefficient (convection) enhancement basis in Nusselt number, and pressure drop basis in Euler number.

3.3. Correlating the FOMs with the FPSC thermal efficiency

The principal aim of this work is assessing the applicability of different nanofluid FOMs in FPSC thermal efficiency. While Sections 3.1 and 3.2 provide in-depth numerical and analytical analyses on thermal efficiency and FOMs for Al_2O_3, TiO_2, SiO_2, polystyrene, GNP, and SWCNT nanofluids; here the relation between the investigated FOMs and thermal efficiency is statistically clarified.

Here FOM's are regarded as raters employed to determine whether an HTF is efficient in an FPSC. FOMs' dependence on thermo-physical properties makes them easier to compute compared to thermal efficiency. Here the raters are Mo_{ratio} (Eq. (1b)), PEC_{ratio} (Eq. (3)), and η (Eq. (4)) along FOMs, and their individual evaluations on (ne-)HTF's are statistically compared to those of FPSC thermal efficiency. As a reminder, each FOM has a specific range to conclude an HTF's applicability, i.e., $Mo_{nf}/Mo_{bf} > 1$, $C_\mu/C_k < 4$, $PEC_{nf}/PEC_{bf} > 1$, $\eta > 1$. To discard the bias caused by the evaluation criteria specific to the FOM, values of Mo_{ratio}, PEC_{ratio} and η distributions, along with the FPSC thermal efficiency are first normalized to the respective values of water, and then within each group to ensure their values are in the range 0–1 with "the greater the better" criterion. C_μ / C_k is disregarded due to its insensitivity to flow condition. The first normalization is due to the fact that since Mo_{ratio}, PEC_{ratio} and η are FOMs that essentially used to compare a ne-HTF with the base fluid, the FPSC thermal efficiency should also include values normalized to those of the base fluid for a proper comparison.

Kendall's *W* (Kendall's Coefficient of Concordance) is a non-parametric measure used to determine the agreement among the raters. Here the task is to compute the Kendall's *W* between a FOM and the FPSC thermal efficiency to statistically assess the compatibility of the specific FOM with the thermal efficiency. For each evaluation, the coefficient can take values in the range 0–1, and the consistency gets better as the value of the coefficient approaches 1. Results are given in

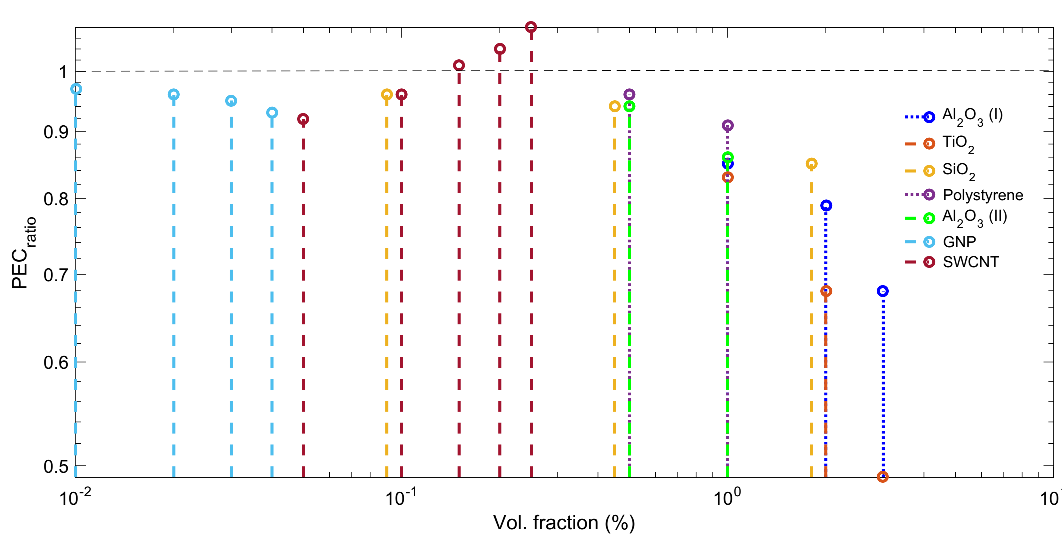

Fig. 7. *PEC* ratio for laminar flow. The horizontal dashed line depicts the *PEC* ratio of water.

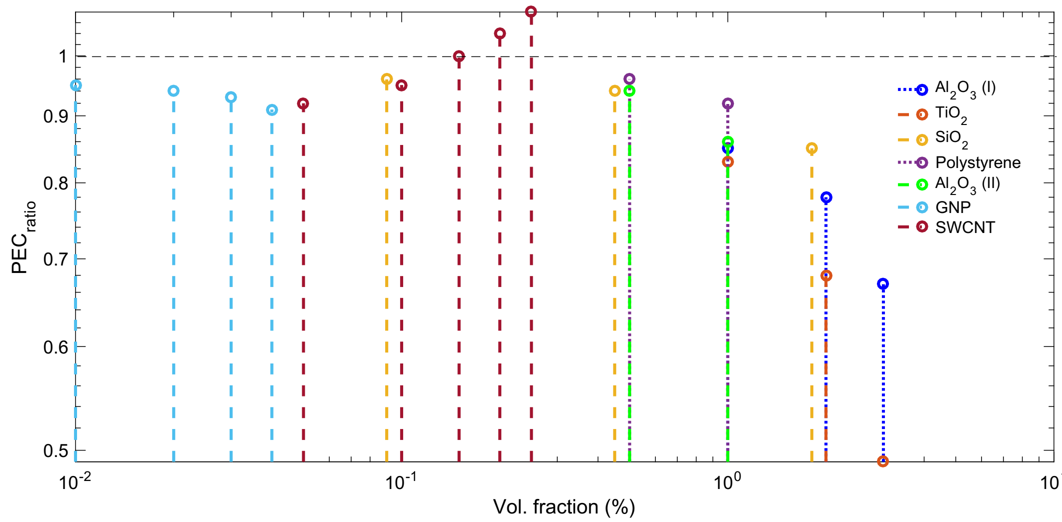

Fig. 8. *PEC* ratio for turbulent flow. The horizontal dashed line depicts the *PEC* ratio of water.

Table 1 for each comparison.

Results presented in Table 1 reveal that the Mo_{ratio} and FPSC thermal efficiencies rate the considered HTF's in a statistically compatible manner, i.e., no statistically significant difference among their rating is observed at 0.05 significance level. In this case, Kendall's $W = 0.853 > 0.80$ suggests a very good consistency level. On the other hand, the normalized η ($p = 0.218 > 0.05$) and normalized PEC_{ratio} ($p = 0.147 > 0.05$) ratings are statistically different than that of the FPSC thermal efficiency.

Results based on this population are evaluated based on "the greater the better" criterion, irrespective of the flow condition or the other parameters used in evaluating the FOM's and system thermal efficiency. Based on the outcomes of the statistical analyses, it can be inferred that the FOMs employed to represent the benefits of an HTF should be application-specific. The difference between η and FPSC thermal efficiency is the greatest (as quantitatively shown in Table 1, with the lowest Kendall's W and the highest p-value); while the results of Mo_{ratio} and FPSC thermal efficiency are the closest among the studied distributions.

4. Conclusions

This work investigates the applicability of different FOMs for the employment of nanofluids as working fluids in heat transfer processes. This evaluation is of critical importance since thermal modeling of systems requires considerable computational power and time, which mostly fail to consider much of the spatial and temporal effects together due to the nature and content of nanofluids. There the ease of applicability of FOMs comes to the fore, as more practical measures to characterize the advantages of a working fluid in a system.

The main outcomes of this work are:

- Thermal efficiency depends on nanoparticle type due to material-dependent thermo-physical properties and heat transfer coefficients, and varies differently with nanoparticle loading for different flow regimes.
- For metal oxide, GNP, and SWCNT nanofluids, efficiency increased with increased nanoparticle fraction, since their improved thermal characteristics' made up for increased hydrodynamic losses due to high viscosity in laminar flow.

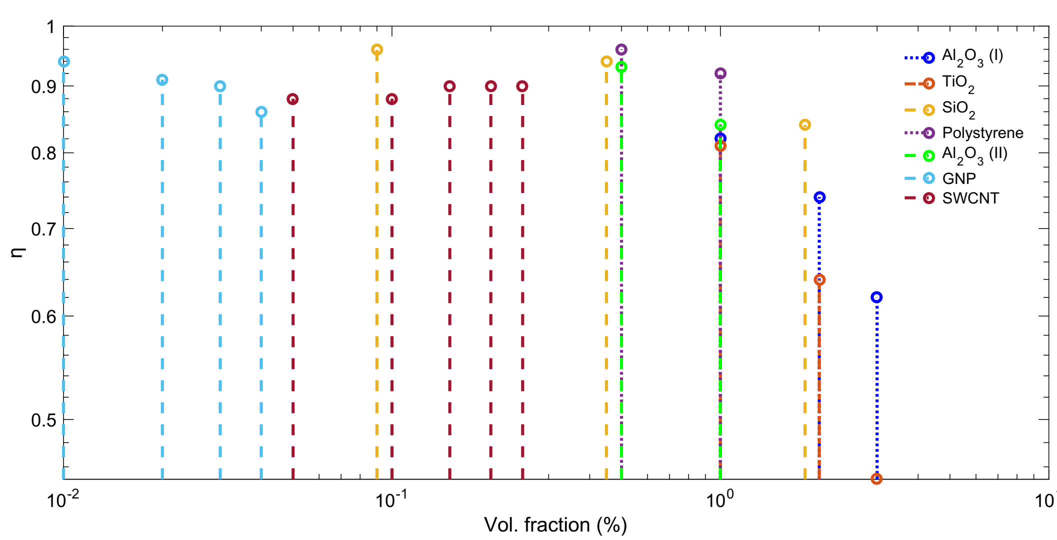

Fig. 9. Results of η for laminar flow.

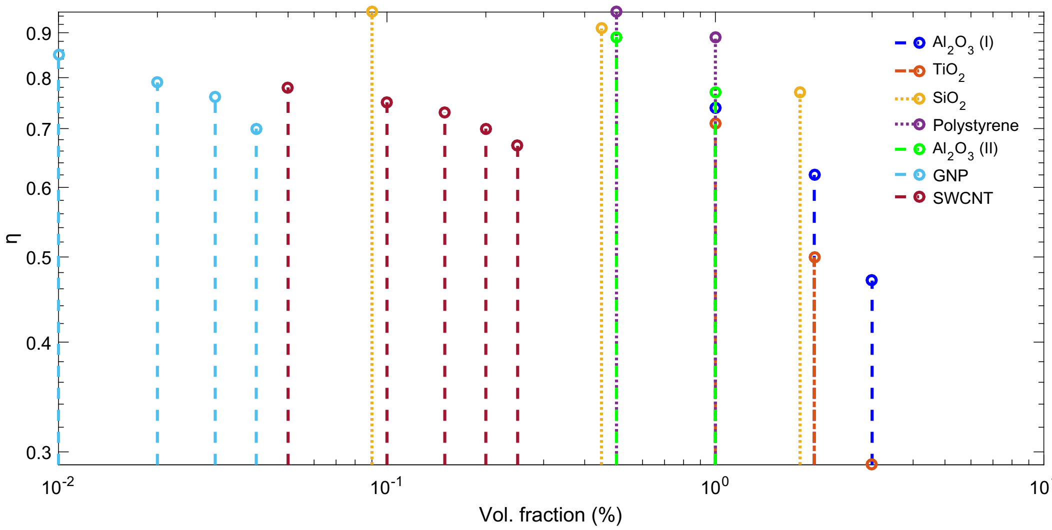

Fig. 10. Results of η for turbulent flow.

- Turbulent flow induces high pressure drops and decreasing thermal efficiencies with increasing nanoparticle fractions for all the ne-HTF's investigated.
- Mo_{ratio} for laminar flow is in the same direction as the thermal efficiency; showing reduced Mo_{ratio} for polystyrene and SiO_2, and increased Mo_{ratio} for the rest of ne-HTF's. Mo_{ratio} is $>$ 1 for Al_2O_3, TiO_2, graphene, and SWCNT; is slightly $<$ 1 for SiO_2, and is $<$ 1 for polystyrene nanofluid; showing that Al_2O_3, TiO_2, graphene, and SWCNT nanofluids in studied concentrations are more advantageous than water.
- Mo_{ratio} for turbulent flow does not fully coincide with the thermal efficiency. Mo_{ratio} increased for GNP, and decreased for all the other ne-HTF's studied with the nanoparticle fraction. On the other hand, the thermal efficiencies of the GNP nanofluids do not change considerably with the nanoparticle fraction.
- Al_2O_3 and TiO_2 ne-HTF's exhibit C_μ / C_k $>$ 4 and appear non-beneficial based on this FOM. C_μ / C_k $<$ 0 case appears for low relative thermal conductivity ne-HTF's. Only GNP and concentrated SWCNT nanofluids C_μ / C_k value is $<$ 4, making them promising HTF's.
- PEC_{ratio}'s are not in agreement with C_μ / C_k and Mo_{ratio} for laminar flow, such that only concentrated SWCNT nanofluids provide PEC_{ratio} $>$ 1 and metal-oxides, SiO_2, and GNP nanofluids PEC ratios decrease as the nanoparticle concentration increases. For turbulent flow, PEC_{ratio} results point out to the same ne-HTF rating as the thermal efficiency.
- Overall energetic efficiency (η) for laminar flow does not provide the advantageous-disadvantageous classification as the FPSC thermal efficiency. This trend is not conserved for turbulent flow, yielding decreased η with the nanoparticle fraction.
- The ER's decrease as the nanoparticle fraction augments both for laminar and turbulent flow, and found non-representative of FPSC thermal efficiency.
- Results of the statistical tests reveal that not all FOMs are applicable to FPSC operation. The type of FOM is important to conclude the effectiveness of an HTF in a specific application, as different merits focused on and point out to different thermal/flow aspects.
- Specific to this work, Mo_{ratio} is determined as a viable merit, while PEC_{ratio} and η are not representative of the FPSC thermal efficiency.
- As a result of the analyses performed in this work, it should be highlighted that FOM selection should be done carefully to represent the application.

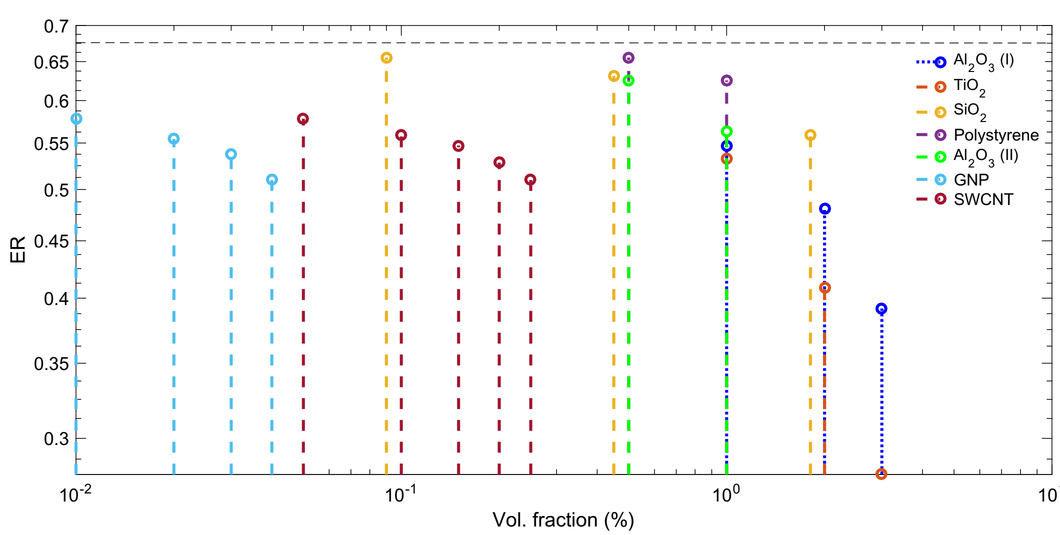

Fig. 11. ER for laminar flow. The horizontal dashed line depicts the ER value of water.

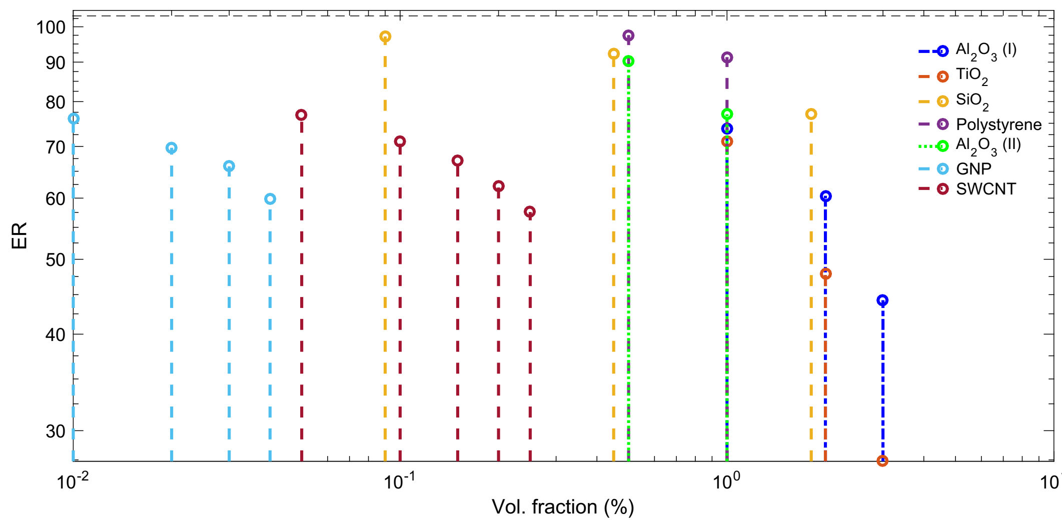

Fig. 12. *ER* for turbulent flow. The horizontal dashed line depicts the *ER* value of water.

Table 1
Kendall's *W* results for individual Mo_{ratio}, η, PEC_{ratio} rating comparisons against FPSC thermal efficiency ratio (all normalized).

Comparison Test Statistics	Thermal efficiency ratio vs. Mo_{ratio}	Thermal efficiency ratio vs. η	Thermal efficiency ratio vs. PEC_{ratio}
N	2	2	2
Kendall's W[a]	0.853	0.570	0.598
Chi-Square	97.192	65.018	68.183
df	57	57	57
p	0.001	0.218	0.147

a. Kendall's Coefficient of Concordance.

CRediT authorship contribution statement

Elif Begum Elcioglu: Formal analysis, Writing - original draft. **Alper Mete Genc:** Software, Investigation. **Ziya Haktan Karadeniz:** Conceptualization, Writing - review & editing. **Mehmet Akif Ezan:** Software, Investigation, Writing - review & editing. **Alpaslan Turgut:** Conceptualization, Supervision.

Declaration of Competing Interest

The authors declare that they have no known competing financial interests or personal relationships that could have appeared to influence the work reported in this paper.

Appendix A. Supplementary data

Supplementary data to this article can be found online at https://doi.org/10.1016/j.enconman.2019.112292.

References

[1] Feynmann R. There's plenty of room at the bottom. Eng Sci 1960;23(5):22–36.
[2] Choi SUS, Eastman JA. Enhancing thermal conductivity of fluids with nanoparticles, in ASME International Mechanical Engineering Congress & Exposition, p. 7 pp.
[3] Raja M, Vijayan R, Dineshkumar P, Venkatesan M. Review on nanofluids characterization, heat transfer characteristics and applications. Renew Sustain Energy Rev 2016;64:163–73.
[4] Ganvir RB, Walke PV, Kriplani VM. Heat transfer characteristics in nanofluid—a review. Renew Sustain Energy Rev 2016;75(November):451–60. 2017.
[5] Gupta M, Singh V, Kumar R, Said Z. A review on thermophysical properties of nanofluids and heat transfer applications. Renew Sustain Energy Rev 2017;74:638–70.
[6] Saidur R, Leong KY, Mohammad HA. A review on applications and challenges of nanofluids. Renew Sustain Energy Rev 2011;15(3):1646–68.
[7] Sidik NAC, Mohammed HA, Alawi OA, Samion S. A review on preparation methods and challenges of nanofluids. Int. Commun. Heat Mass Transf. 2014;54:115–25.
[8] Sarkar J, Ghosh P, Adil A. A review on hybrid nanofluids: recent research, development and applications. Renew Sustain Energy Rev 2015;43:164–77.
[9] Mouromtseff IE. Water and forced-air cooling of vacuum tubes* nonelectronic problems in electronic tubes. In: Proceedings of the I. R. E., 1942, no. April, pp. 190–205.
[10] Prasher R, Song D, Wang J, Phelan P. Measurements of nanofluid viscosity and its implications for thermal applications. Appl Phys Lett 2006;89(133108):1–3.
[11] Sekrani G, Poncet S, Proulx P. Modeling of convective turbulent heat transfer of water-based Al_2O_3 nanofluids in an uniformly heated pipe. Chem Eng Sci 2018;176:205–19.
[12] Ferrouillat S, Bontemps A, Ribeiro J-P, Gruss J-A, Soriano O. Hydraulic and heat transfer study of SiO_2/water nanofluids in horizontal tubes with imposed wall temperature boundary conditions. Int J Heat Fluid Flow 2011;32(2):424–39.
[13] Sharifpur M. Nanofluids; opportunities, lack of principle research and points on accurate publications (plenary lecture), in ICNF 2019, 2019.
[14] Alirezaie A, Hajmohammad MH, Alipour A, Salari M. Do nanofluids affect the future of heat transfer? "A benchmark study on the efficiency of nanofluids". Energy 2018;157:979–89.
[15] Allouhi A, Amine MB, Saidur R, Kousksou T, Jamil A. Energy and exergy analyses of a parabolic trough collector operated with nanofluids for medium and high temperature applications. Energy Convers Manage 2018;155:201–17.
[16] Yasinskiy A, et al. Dramatically enhanced thermal properties for TiO_2-based nano fluids for being used as heat transfer fluids in concentrating solar power plants. Renew Energy 2018;119:809–19.
[17] Gómez-Villarejo R, et al. Ag-based nanofluidic system to enhance heat transfer fluids for concentrating solar power: nano-level insights. Appl Energy 2017;194:19–29.
[18] Tong Y, Lee H, Kang W, Cho H. Energy and exergy comparison of a flat-plate solar collector using water, Al_2O_3 nanofluid, and CuO nanofluid. Appl Therm Eng 2019;159:113959.
[19] Mirzaei M, Hosseini SMS, Kashkooli AMM. Assessment of Al_2O_3 nanoparticles for the optimal operation of the flat plate solar collector. Appl Therm Eng 2018;134:68–77.
[20] Hawwash AA, Abdel Rahman AK, Nada SA, Ookawara S. Numerical investigation and experimental verification of performance enhancement of flat plate solar collector using nanofluids. Appl Therm Eng 2018;130:363–74.
[21] Shojaeizadeh E, Veysi F. Development of a correlation for parameter controlling using exergy efficiency optimization of an Al_2O_3/water nanofluid based flat-plate solar collector. Appl Therm Eng 2016;98:1116–29.
[22] Colangelo G, Favale E, De Risi A, Laforgia D. A new solution for reduced sedimentation flat panel solar thermal collector using nanofluids. Appl Energy 2013;111:80–93.
[23] Genc AM, Ezan MA, Turgut A. Thermal performance of a nanofluid-based flat plate solar collector: a transient numerical study. Appl Therm Eng 2018;130:395–407.
[24] Saffarian MR, Moravej M, Doranehgard MH. Heat transfer enhancement in a flat plate solar collector with different flow path shapes using nanofluid. Renew Energy 2020;146:2316–29.
[25] He Q, Zeng S, Wang S. Experimental investigation on the efficiency of flat-plate solar collectors with nanofluids. Appl Therm Eng 2014;88:165–71.
[26] Moghadam AJ, Farzane-Gord M, Sajadi M, Hoseyn-Zadeh M. Effects of CuO/water nanofluid on the efficiency of a flat-plate solar collector. Exp Therm Fluid Sci 2014;58:9–14.
[27] Sint NKC, Choudhury IA, Masjuki HH, Aoyama H. Theoretical analysis to determine the efficiency of a CuO-water nanofluid based-flat plate solar collector for domestic solar water heating system in Myanmar. Sol Energy 2017;155:608–19.
[28] Mirzaei M. Experimental investigation of CuO nanofluid in the thermal characteristics of a flat plate solar collector. Environ Prog Sustain Energy 2019;38(1):260–7.

[29] Salavati Meibodi S, Kianifar A, Niazmand H, Mahian O, Wongwises S. Experimental investigation on the thermal efficiency and performance characteristics of a flat plate solar collector using SiO_2/EG-water nanofluids. Int Commun Heat Mass Transf 2015;65:71–5.
[30] Kiliç F, Menlik T, Sözen A. Effect of titanium dioxide/water nanofluid use on thermal performance of the flat plate solar collector. Sol Energy 2018;164:101–8.
[31] Sadeghzadeh M, Ahmadi MH, Kahani M, Sakhaeinia H, Chaji H, Chen L. Smart modeling by using artificial intelligent techniques on thermal performance of flat – plate solar collector using nanofluid. Energy Sci Eng 2019:1–10.
[32] Farajzadeh E, Movahed S, Hosseini R. Experimental and numerical investigations on the effect of Al_2O_3/TiO_2-H_2O nanofluids on thermal efficiency of the flat plate solar collector. Renew Energy 2018;118:122–30.
[33] Sharafeldin MA, Gróf G. Experimental investigation of flat plate solar collector using CeO_2-water nanofluid. Energy Convers Manage 2018;155:32–41.
[34] Yousefi T, Shojaeizadeh E, Veysi F, Zinadini S. An experimental investigation on the effect of pH variation of MWCNT-H_2O nanofluid on the efficiency of a flat-plate solar collector. Sol Energy 2012;86(2):771–9.
[35] Ahmadi A, Ganji DD, Jafarkazemi F. Analysis of utilizing graphene nanoplatelets to enhance thermal performance of flat plate solar collectors. Energy Convers Manage 2016;126:1–11.
[36] Verma SK, Tiwari AK, Tiwari S, Chauhan DS. Performance analysis of hybrid nanofluids in flat plate solar collector as an advanced working fluid. Sol Energy 2018;167:231–41.
[37] Sharafeldin MA, Gróf G, Mahian O. Experimental study on the performance of a flat-plate collector using WO_3/Water nanofluids. Energy 2017;141:2436–44.
[38] Otanicar T, Phelan PE, Prasher RS, Rosengarten G, Taylor RA. Nanofluid-based direct absorption solar collector. J Renew Sustain Energy 2010;2(033102).
[39] Hazra SK, Ghosh S, Nandi TK. Photo-thermal conversion characteristics of carbon black-ethylene glycol nanofluids for applications in direct absorption solar collectors. Appl Therm Eng 2019;163:114402.
[40] Sarsam WS, Kazi SN, Badarudin A. A review of studies on using nanofluids in flat-plate solar collectors. Sol Energy 2015;122:1245–65.
[41] Goel N, Taylor RA, Otanicar T. A review of nano fluid-based direct absorption solar collectors: design considerations and experiments with hybrid PV/Thermal and direct steam generation collectors. Renew Energy 2020;145:903–13.
[42] Eltaweel M, Abdel-Rehim AA. Energy and exergy analysis of a thermosiphon and forced-circulation flat-plate solar collector using MWCNT/water nanofluid. Case Stud Therm Eng 2019;14:100416.
[43] Verma SK, Tiwari AK, Chauhan DS. Performance augmentation in flat plate solar collector using MgO/water nanofluid. Energy Convers Manage 2016;124:607–17.
[44] Verma SK, Tiwari AK, Chauhan DS. Experimental evaluation of flat plate solar collector using nanofluids. Energy Convers Manage 2017;134:103–15.
[45] Yu W, France DM, Timofeeva EV, Singh D, Routbort JL. Comparative review of turbulent heat transfer of nanofluids. Int J Heat Mass Transf 2012;55:5380–96.
[46] Suganthi KS, Rajan KS. Metal oxide nanofluids: review of formulation, thermo-physical properties, mechanisms, and heat transfer performance. Renew Sustain Energy Rev 2017;76:226–55.
[47] Buschmann MH, et al. Correct interpretation of nanofluid convective heat transfer. Int J Therm Sci 2018;129:504–31.
[48] Garg J, et al. Enhanced thermal conductivity and viscosity of copper nanoparticles in ethylene glycol nanofluid. J Appl Phys 2008;103(7):074301.
[49] Genc AM, Elcioglu EB, Karadeniz ZH, Ezan MA, Turgut A, Solar radiation harvesting via flat plate collectors : nanofluid figure of merit against thermal efficiency. In: 1st International Conference on Nanofluids (ICNf2019) and 2nd European Symposium on Nanofluids (ESNf2019), 2019.
[50] Timofeeva E, Yu W, France DM, Singh D, Routbort JL. Nanofluids for heat transfer : an engineering approach. Nanoscale Res Lett 2011;6(182):1–7.
[51] Vajjha RS, Das DK. A review and analysis on influence of temperature and concentration of nanofluids on thermophysical properties, heat transfer and pumping power. Int J Heat Mass Transf 2012;55:4063–78.
[52] Turgut A, Sağlanmak Ş, Doğanay S. Experimental investigation on thermal conductivity and viscosity of nanofluids: particle size effect. J Fac Eng Archit Gazi Univ 2016;31(1):95–103.
[53] Turgut A, Tavman I, Chirtoc M, Schuchmann HP, Sauter C, Tavman S. Thermal conductivity and viscosity measurements of water-based TiO_2 nanofluids. Int J Thermophys 2009;30:1213–26.
[54] Mikkola V, Puupponen S, Granbohm H, Saari K, Seppälä A. Influence of particle properties on convective heat transfer of nanofluids. Int J Therm Sci 2018;124:187–95.
[55] Iranmanesh S, Chyuan H, Chin B, Sadeghinezhad E, Esmaeilzadeh A, Mehrali M. Thermal performance enhancement of an evacuated tube solar collector using graphene nanoplatelets nano fluid. J Clean Prod 2017;162:121–9.
[56] Sabiha MA, Mostafizur RM, Saidur R, Mekhilef S. Experimental investigation on thermo physical properties of single walled carbon nanotube nanofluids. Int J Heat Mass Transf 2016;93:862–71.
[57] Mondragón R, Sánchez D, Cabello R, Llopis R, Juliá JE. Flat plate solar collector performance using alumina nanofluids: experimental characterization and efficiency tests. PLoS ONE 2019;14(2):1–18.
[58] Minea AA. Comparative study of turbulent heat transfer of nanofluids: Effect of thermophysical properties on figure-of-merit ratio. J Therm Anal Calorim 2016;124(1):407–16.